Research Square

Preprints are preliminary reports that have not undergone peer review.
They should not be considered conclusive, used to inform clinical practice,
or referenced by the media as validated information.

Global evaluation of Overture Maps reveals source-driven disparities in urban geospatial data

Levente Juhász

levente.juhasz@ufl.edu

University of Florida

Hartwig H. Hochmair

University of Florida

Article

Keywords:

Posted Date: November 2nd, 2026

DOI: https://doi.org/10.21203/rs.3.rs-11038658/v1

License: This work is licensed under a Creative Commons Attribution 4.0 International License.
Read Full License

Additional Declarations: No competing interests reported.

Global evaluation of Overture Maps reveals source-driven disparities in urban geospatial data

Levente Juhász[1,2,*,†] and Hartwig H. Hochmair[1,†]

[1] Fort Lauderdale Research and Education Center, School of Forest, Fisheries and Geomatics Sciences, University of Florida, Davie, FL, USA
[2] Geospatial Analytics, Technology and Open Research (GATOR) Lab, University of Florida, Davie, USA

* Author to whom correspondence should be addressed (levente.juhasz@ufl.edu)
† These authors contributed equally to this work.

Levente Juhász, levente.juhasz@ufl.edu, ORCID: https://orcid.org/0000-0003-3393-4021
Hartwig H. Hochmair, hhhochmair@ufl.edu, ORCID: https://orcid.org/0000-0002-7064-8238

Abstract

Open geospatial platforms aggregating data from multiple providers support urban analytics worldwide, yet the quality implications of global-scale conflation remain poorly understood. We assess Overture Maps data quality across two releases (November 2024, April 2026) for 11,422 GHSL-defined urban areas. Point-of-interest coordinate duplication improved from a city-level median of 27.5% to 8.7% between releases, driven mainly by Meta's internal deduplication. Building attribute completeness is and remains low globally: only 9% of buildings carry any semantic attribute, and height data is absent entirely for nearly three-quarters of cities. Binomial mixed-effects models of building completeness and precision across 320 sampled cities show that source composition is the strongest predictor of data quality. A greater OpenStreetMap share is associated with greater completeness, whereas greater Google and Microsoft shares are associated with lower completeness and precision. The effects are concentrated in the global South regions where machine learning-derived sources currently predominate. Data users should treat the contributing source, rather than release version, as the primary quality diagnostic when selecting Overture data for downstream applications.

Urban areas now house about 55% of the world's population[1] and generate a disproportionate share of global economic activity[2,3], making high-quality, spatially explicit geospatial data essential for navigation, logistics, emergency response, and sustainability planning. Building footprints and points of interest (POIs) are primary inputs for location-based services, urban analytics, and infrastructure modeling[4,5], and underpin built environment morphology characterization[6], climate-related hazard exposure estimation[7], and population mapping where census data are absent[8]. Although integrating heterogeneous datasets helps reduce geographic disparities in coverage, substantial spatial biases persist in completeness, thematic accuracy, and positional consistency[9,10]. The Overture Maps Foundation (OMF), established in 2022 by a consortium of technology and mapping companies, represents the first large-scale industry effort to produce a globally normalized, openly licensed alternative to OpenStreetMap

(OSM), consolidating contributions from more than 30 commercial and public-sector providers into a unified schema[11–13]. By the April 2026 release, OMF's global catalogue comprised approximately 66 million POIs and 585 million building footprints. This scale makes systematic, independent quality auditing both essential and methodologically demanding.

The quality of open and crowdsourced spatial datasets has been studied extensively for OSM[14], the most comparable freely available global dataset. Global building completeness assessments have documented pronounced geographic disparities[15]: a spatio-temporal analysis across 13,189 cities found an average OSM building completeness of 24%, substantially higher in Europe and North America than in Sub-Saharan Africa and Southern Asia[16]. Similar patterns emerge from proxy-based assessments at comparable scale[17] and from crowdsourced validation[18], consistently linking completeness gaps to socioeconomic context and mapping activity. POI quality has been evaluated across multiple platforms and urban regions, revealing persistent differences in category assignment depth, provider prominence, and spatial consistency between datasets[19–22]. Volunteered geographic information[9] (VGI) quality reviews have formalized the distinction between intrinsic indicators (derivable from the dataset itself), and extrinsic indicators (requiring an independent ground truth), highlighting completeness and thematic accuracy as most sensitive to geographic context[10,23]. For building data and large-scale conflation efforts, increasing machine-learning contributions lowers geometric quality but reduces geographic inequality compared to community-edited data[24,25].

For Overture specifically, the evidence base remains geographically limited. A UK-focused assessment of Overture Places found high completeness and positional accuracy but mixed thematic quality, where source-specific gaps, such as missing category attributes for Microsoft-sourced POIs, persisted after conflation[26]. An evaluation of Overture building footprints in Tanzania and the Philippines reported lower-than-expected accuracies and representation biases linked to population density and socioeconomic indicators[27]. More recent studies confirm growing adoption of Overture data[11,28]; yet, no study has assessed its quality across cities globally, evaluated changes following major pipeline updates, or examined how source composition mediates regional disparities across geographies and thematic domains.

Our study presents a global, multi-theme quality assessment of Overture Maps across the November 2024 and April 2026 releases. Under the ISO 19157 geographic data quality framework, intrinsic quality metrics such as source diversity, positional co-location, and category specificity for places; and attribute completeness, geometric overlap for buildings were computed for 11,422 GHSL-defined urban areas; extrinsic completeness and precision were evaluated against ground-truth building counts for a stratified sample of 338 cities across nine world regions. We show that POI quality (positional accuracy, category information) improved substantially between releases, that building attribute information remains sparse irrespective of data release, and that geographic divergence in building completeness and precision is at least partially driven by source composition.

Results

Intrinsic measures: Place data

The Overture Places dataset grew by 37.0%, from 30.9 million to 42.4 million features within GHSL-defined urban areas between the November 2024 and April 2026 releases (55.7% and 56.1% of Overture's total global POI inventory, respectively), with growth observed across all nine world regions (Table S1.2). Growth was most pronounced in Latin America and the Caribbean (LAC, 46.6%) and Europe (44.9%), while Sub-Saharan Africa (SSA) recorded the smallest relative increase (2.0%).

In 2024, Overture Places drew from two sources: Meta (90.7% of all features) and Microsoft (9.3%), with a global city-level median of two unique sources per urban area (Table S1.2). By 2026, eight providers contributed to the global dataset, with Meta remaining the largest contributor (80.7%) and Foursquare[29] emerging as the second-largest contributor at 8.6% of all features. The remaining contributors in the 2026 release were Microsoft (8.4%), AllThePlaces[30] (2.0%) and four minor providers collectively contributing less than 0.5% (Table 1, Table S1.5). Meta's decline in global share reflects the expanded data contributor base rather than a reduction in Meta's absolute footprint, which grew by 21.9% over the same period. Source diversification was, however, geographically uneven when measured by Pielou's evenness index (E) (Fig. 1). While evenness increased from 0.09 to 0.24 globally, cities in Northern America (NA, median E = 0.55), Australia and New Zealand (ANZ, E = 0.52), and Europe (E = 0.48) achieved the most balanced multi-provider coverage by 2026, whereas urban areas across SSA (E = 0.09), Northern Africa and Western Asia (NAWA, E = 0.08), and LAC (E = 0.12) remained near-exclusively dependent on Meta. The eight contributing providers thus reflect a geographically concentrated expansion and not a uniform improvement in source diversity.

Positional co-location (POIs sharing identical coordinates) improved notably between releases. The proportion of POIs co-located with at least one other POI declined from a city-level median of 27.5% in 2024 to 8.7% in 2026, with the median of the maximum co-location stack across cities falling from 27 to 8 (Fig. 2).The improvement was driven primarily by Meta, one of two major data providers in both releases. All six providers introduced in 2026 recorded median co-location rates of 0.0% from the onset (Table 1, Table S1.5).

POI category information also improved substantially as the global median share of uncategorized POIs with null category values declined more than fourfold, from 14.3% in 2024 to 3.1% in 2026 (Table S1.2; Fig. S1.1). Where categories were assigned, they also became more granular: the specificity score ($S_k \in [0, 1]$, Supplementary Materials §3) increased from a global city-level median of 0.690 to 0.777. This indicates that the decline in uncategorized POIs was accompanied by more precise labelling, rather than merely by the addition of coarse top-level categories (Fig. S1.2, Table S1.2).

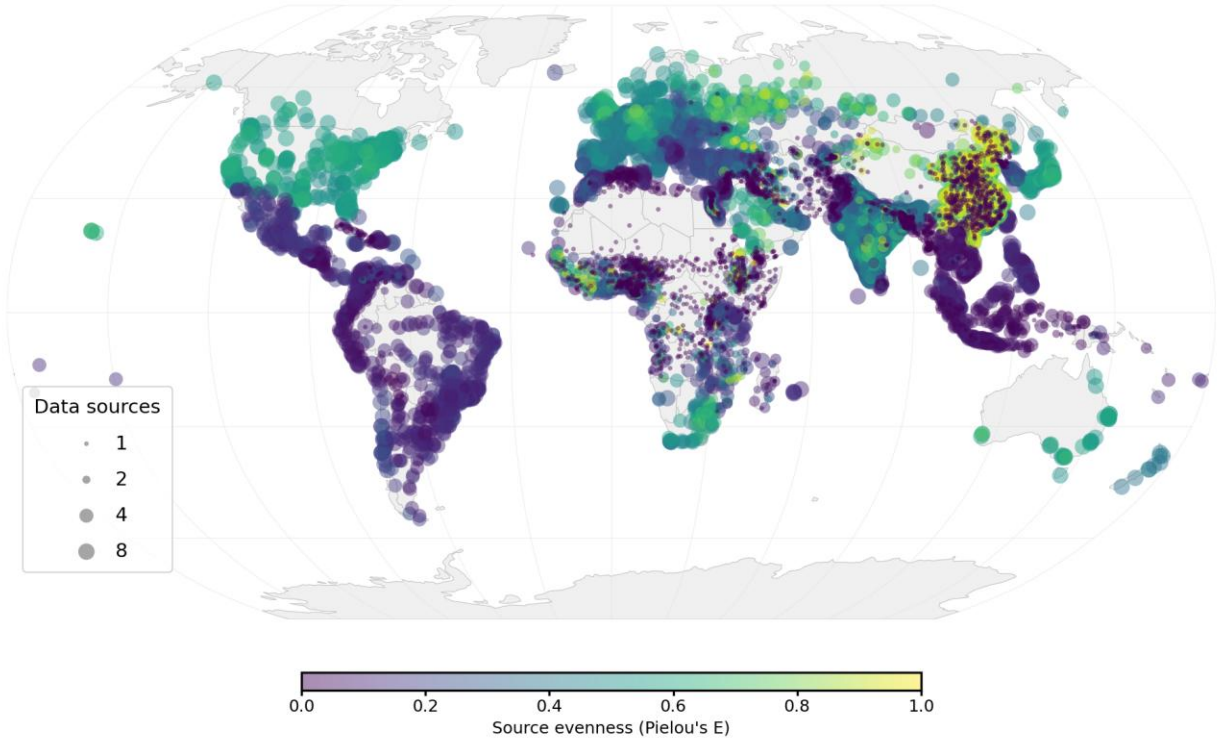


Fig. 1. Source diversity of Overture Places by city in 2026. Each point represents one of 11,422 GHSL-defined urban areas. Dot color encodes Pielou's evenness index, from single-source monopoly (E = 0, purple) to balanced multi-source coverage (E = 1, yellow); dot size is proportional to the number of contributing sources.

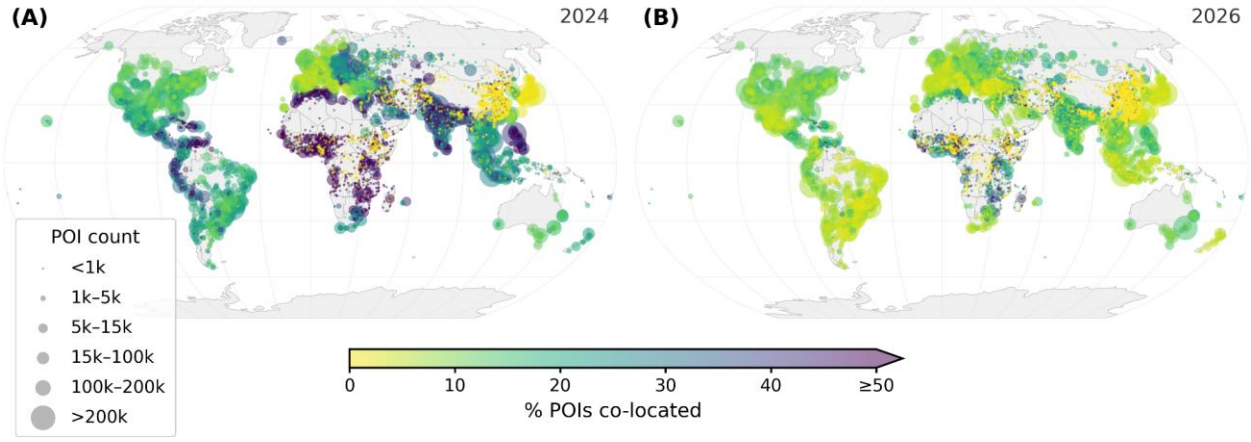


Fig. 2. POI position co-location by city for November 2024 (A) and April 2026 (B). Each point represents one GHSL urban area. Color encodes the co-location proportion, from no co-location (0%, yellow) to high co-location (≥50%, purple); dot size is proportional to total POI count.

The improvements reclect two factors: Meta's 2026 product update and new data sources such as Foursquare, which entered with near-zero co-location and near-complete category assignment (Table S1.5). Hence, in geographic regions that remained near-exclusively Meta-dependent, such as Central and Southern Asia (CSA), Meta data quality improvements had the largest effect.

Table 1. Intrinsic quality of Overture Places by data source and data release, computed across GHSL-defined urban areas (*n*=11,422). Values report city-level median (mean). Δ rows show change in corresponding quality measures between releases for sources present in both releases. Changes for five minor sources are reported in Table S1.5.

				P-02 (Co-location)		P-03 (Category Quality)	
Source	**Year**	**Number of POIs**	**% Share**	**Max Stack**	**% Co-located**	**% Null Category**	**Specificity (S_k)**
Meta	2026	34,210,503	80.7	8.0 (19.4)	7.0 (11.3)	2.4 (3.7)	0.77 (0.77)
	2024	28,060,629	90.7	27.0 (46.1)	28.6 (31.0)	14.1 (16.3)	0.68 (0.69)
	Δ	+6,149,874	-10.0%	-19.0 (-26.7)	-21.6 (-19.7)	-11.7 (-12.6)	+0.09 (+0.08)
Foursquare	2026	3,624,565	8.6	1.0 (2.3)	0.0 (3.1)	1.9 (4.5)	0.82 (0.77)
Microsoft	2026	3,581,070	8.4	1.0 (5.2)	0.0 (6.2)	6.9 (10.0)	0.85 (0.83)
	2024	2,884,490	9.3	1.0 (4.8)	0.0 (5.6)	11.8 (15.5)	0.85 (0.83)
	Δ	+696,580	-0.9%	0.0 (+0.4)	0.0 (+0.6)	-4.9 (-5.5)	0.0 (0.0)

Intrinsic measures: Building data

The Overture Buildings dataset comprised 550.4 million features across 11,422 GHSL-defined urban areas in the November 2024 release, growing by 6.2% to 584.5 million features by April 2026 (Table S1.3). In 2024, four sources contributed globally: Google Open Buildings[31] (39.6%), OpenStreetMap (OSM, 35.2%), Microsoft ML Buildings[32] (24.7%), and Esri Community Maps (0.5%). By 2026, three additional sources had been incorporated: the East Asian Buildings dataset[33] (EAB; 6.9%), Instituto Geográfico Nacional de España (IGN, 0.1%), and City of Vancouver (<0.1%), bringing the total to seven contributors. OSM became the most frequent majority source globally in 2026 (36.4%), as Google's share declined from 39.6% to 33.9% despite still acting as the predominant source in most (*n*=4,102) cities (Fig. 3). The EAB addition drove a geographic recomposition in Eastern and South-Eastern Asia (ESEA), where it emerged as the second-largest building source (29.3%), behind OSM (36.4%), displacing Google. City-level source evenness remained relatively low in both releases (median E = 0.507 in 2024, 0.532 in 2026), reflecting persistent single-source dominance in most urban areas globally.

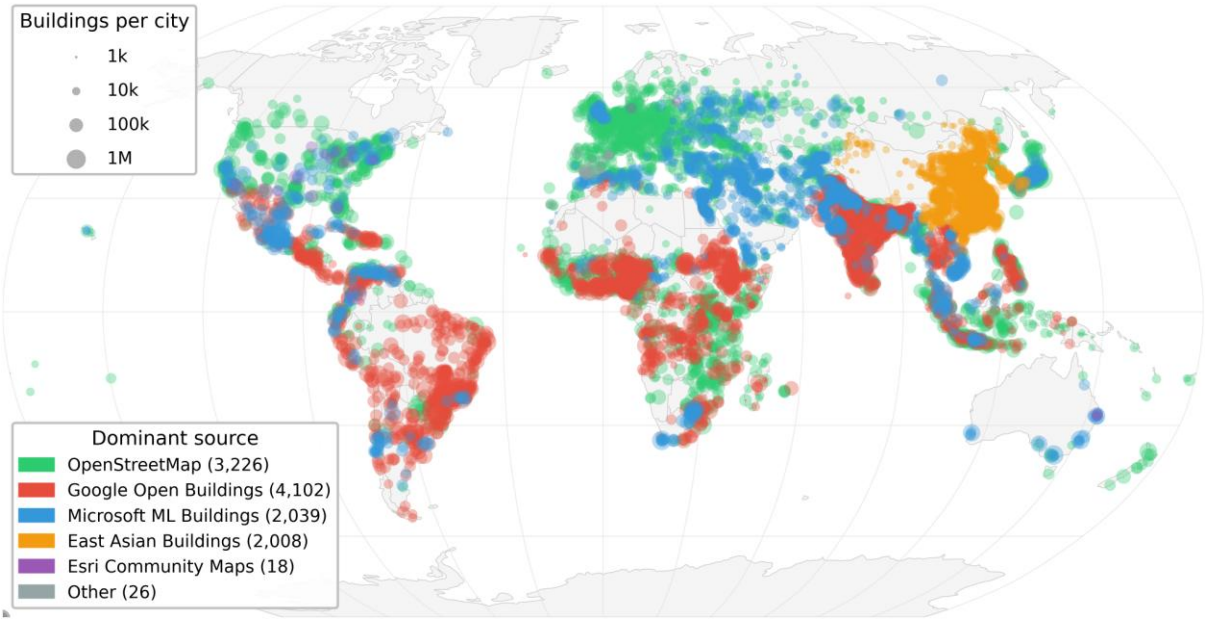


Fig. 3. Dominant building data source by city, April 2026. Each dot represents one GHSL urban area; dot size is proportional to building count; color indicates the majority source.

Attribute completeness was missing almost entirely across all data sources. Google and EAB carried no subtype or floor count information and negligible height data (<0.1%). Microsoft provided no subtype or floor attributes, with algorithmically estimated heights for 9.9% of its features. Only OSM, which contributed 36.4% of all the buildings in the 2026 release carried substantive attribute completeness: 24.7% of OSM buildings included a recorded subtype and 20.0% included height information. Esri, which contributes 0.8% of global features, achieved 10.1% subtype and 25.4% height completeness in 2026 (Table 2). While Esri buildings experienced some notable changes (in both directions) in attribute completeness between both releases, numbers were fairly stable for the other sources demonstrating no improvement in data quality over time in this aspect.

Table 2. Intrinsic quality of Overture Buildings by data source and data release (*n*=11,422 GHSL urban areas). Values are global source-level totals. Geometric overlap (B-03) is not attributable per source and is reported by region in Table S1.3. Two minor sources (IGN, City of Vancouver) are omitted (see Table S1.6).

Source	Year	Buildings (n)	% Share	% Subtype	% Height	% Num Floors
OpenStreetMap	2026	212,873,919	36.4	24.7	20.0	7.7
OpenStreetMap	2024	193,793,572	35.2	24.0	20.8	7.3
	Δ	+19,080,347	+1.2%	+0.7%	-0.8%	+0.4%
Google Open Buildings	2026	198,001,750	33.9	0	0	0
Google Open Buildings	2024	218,004,709	39.6	0	0	0
	Δ	-10,002,959	-5.7%	-	-	-
Microsoft ML Buildings	2026	128,299,981	22.0	0	9.9	0
Microsoft ML Buildings	2024	135,967,213	24.7	0	11.7	0
	Δ	-7,667,232	-2.7%	-	-1.8%	-
East Asian Buildings (EAB)	2026	40,079,233	6.9	0	0	0
Esri Community Maps	2026	4,434,574	0.8	10.1	25.4	4.8
Esri Community Maps	2024	2,622,106	0.5	3.1	58.8	12
	Δ	+1,812,468	+0.3%	+7%	-33.5%	-7.2%

Geometric overlap between building features showed pronounced regional variation in 2026. LAC exhibited the highest rates (median=20.2%), followed by CSA (16.6%) and SSA (9.0%), while Europe (0.6%) and NA (0.1%) recorded near-negligible rates. The more than 50-fold gap between LAC and NA reflects both the greater prevalence of machine learning (ML)-derived building footprints in rapidly urbanizing, high-density regions where footprint delineation is particularly challenging. Globally, median overlap declined slightly from 7.5% to 6.0% between releases (Table S1.3).

Extrinsic measures for Buildings data: completeness and precision

Regional pooled estimates

Table 3 summarizes pooled building data quality by region for the stratified sample of 338 cities, showing completeness and precision based on aggregated counts of true positives, omissions, and commissions across cities in each region. Pooled completeness was calculated as total true positives divided by total reference buildings, and pooled precision as total true positives divided by all mapped buildings. The bracketed values are bootstrap-based 95% confidence intervals obtained by resampling cities within each region.

NA shows the highest performance overall, with very high completeness (0.961) and precision (0.980). Europe also performs strongly, with high completeness (0.950) and precision (0.930). At the other extreme, Oceania has by far the lowest completeness (0.696), though its precision remains high at 0.949, suggesting conservative mapping in which many true buildings are missed but comparatively few false buildings are included. CSA and ESEA also show low completeness (0.825 and 0.865) and precision (0.874 and 0.907). NAWA stands out for low completeness (0.801) despite high precision (0.943), indicating a similar pattern of omission-dominated underrepresentation as for Oceania.

Table 3. Pooled building completeness and precision by world region with bootstrap 95% confidence intervals

Region	Cities (n)	Completeness	Precision
Australia and New Zealand (ANZ)	40	0.925 [0.900, 0.948]	0.981 [0.973, 0.988]
Central and Southern Asia (CSA)	40	0.825 [0.751, 0.884]	0.874 [0.839, 0.900]
Eastern and South-Eastern Asia (ESEA)	40	0.865 [0.770, 0.924]	0.907 [0.862, 0.934]
Europe	40	0.950 [0.929, 0.967]	0.930 [0.902, 0.953]
Latin America and the Caribbean (LAC)	40	0.919 [0.905, 0.932]	0.922 [0.908, 0.935]
Northern Africa and Western Asia (NAWA)	40	0.801 [0.720, 0.870]	0.943 [0.920, 0.960]
Northern America (NA)	40	0.961 [0.940, 0.978]	0.980 [0.974, 0.986]
Oceania	18	0.696 [0.471, 0.864]	0.949 [0.913, 0.973]
Sub-Saharan Africa (SSA)	40	0.944 [0.933, 0.954]	0.893 [0.873, 0.909]

Model-based analysis of completeness

A binomial mixed-effects model (Table S6.1) showed that population density was positively associated with completeness ($\beta = 0.120$, $p < 0.001$), and that source composition was a significant predictor: higher OSM share was associated with greater completeness ($\beta = 0.020$, p

< 0.001), while higher Google (β = −0.216, p < 0.001) and Microsoft (β = −0.049, p < 0.001) shares were associated with lower completeness; EAB was not significant. Relative to Europe, LAC and SSA had significantly higher model-adjusted completeness, and large metropolitan areas showed lower completeness than small urban areas. Tukey-adjusted pairwise comparisons (Fig. S6.1) showed that SSA and LAC had significantly higher completeness than several lower-performing regions, especially ESEA, NAWA, and CSA.

Model-based analysis of precision

A binomial mixed-effects model for precision (Table S6.2) showed population density negatively associated with precision (β = −0.112, p < 0.001), which contrasts with its positive role in completeness. This is, however, consistent with denser built environments presenting more complex geometry where ML footprint delineation is less precise even where coverage is high. Relative to Europe, Central and Southern Asia (β = −1.040, p = 0.019) and Eastern and South-Eastern Asia (β = −1.647, p < 0.001) had significantly lower model-adjusted precision; all larger settlement categories showed lower precision than small urban areas. Among source composition terms, an increase in Microsoft share relative to the aggregated ESRI and IGN component was associated with lower precision *(β* = −0.026, p < 0.001), consistent with ML-derived footprints being geometrically less accurate in complex built environments. The EAB coordinate partly offset the ESEA precision deficit (β = -1.647, p < 0.001). Tukey-adjusted pairwise comparisons (Fig. S6.2) showed that ESEA formed the lowest group by itself, whereas Europe, NAWA, NA, and ANZ formed the highest group.

Global predictions and model validation

Predicted completeness and precision were generated for 11,404 urban settlements (Oceania excluded) from fixed-effects model predictions, allowing extrapolation to countries absent from the training data (see Methods). The resulting global maps (Figs. 4 and 5) show that modelled completeness exhibits a wider range than modelled precision, however with a larger share of cities worldwide falling into the high-end range of completeness than for precision.

Country-level grouped cross-validation (10 folds; see Supplementary Material §6.3) in which all cities from a given country were assigned to the same fold, provided a more conservative assessment than city-level cross-validation because it evaluates transfer to entirely unseen countries. Mean RMSE and MAE were 0.174 and 0.112 for completeness, corresponding to typical errors of approximately 17 and 11 percentage points, and 0.117 and 0.074 for precision, (~12 and 7 percentage points), indicating that the models generalize reasonably well to countries excluded from model fitting.

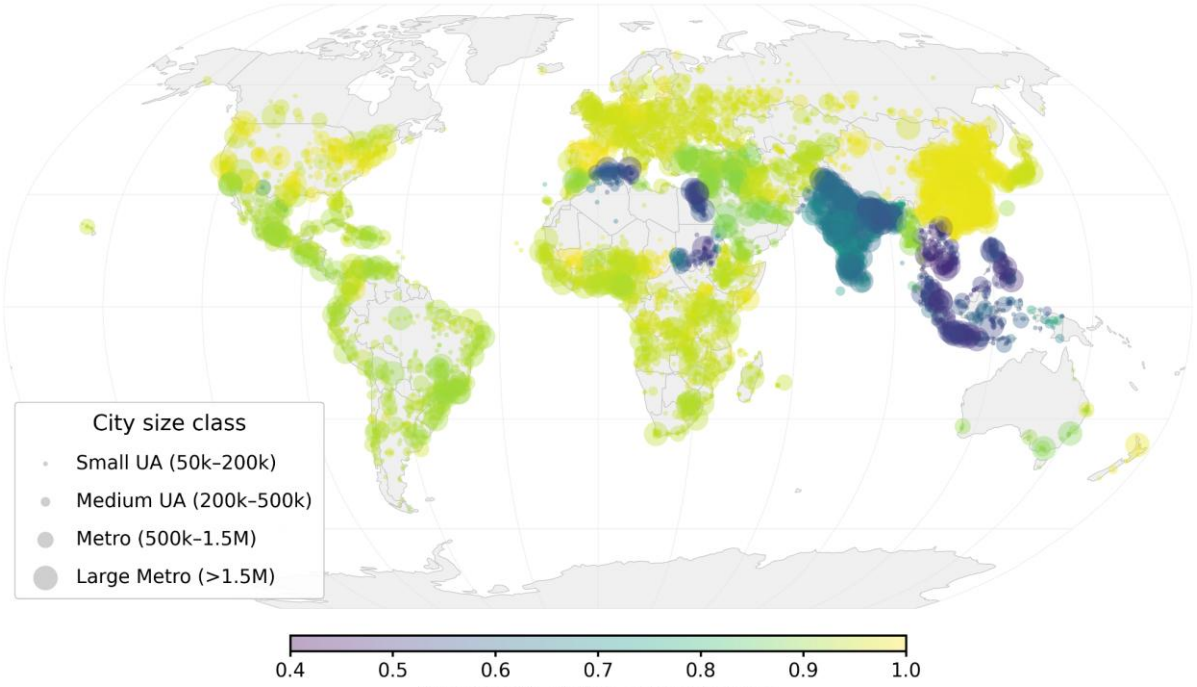


Fig. 4. Predicted building completeness for worldwide urban areas (April 2026). Predictions derived from the binomial mixed-effects model (Table S6.1) using fixed effects only. Dot color encodes predicted completeness (0–1); dot size is proportional to urban classification tier.

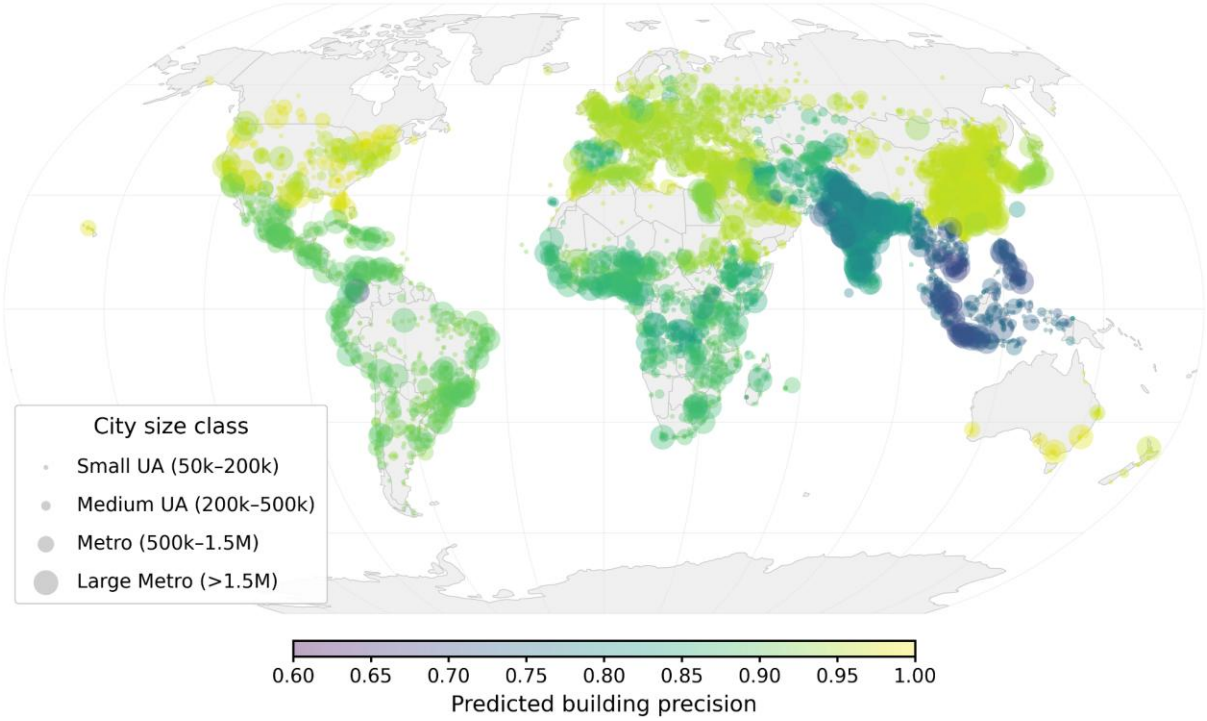


Fig. 5. Predicted building precision for worldwide urban areas (April 2026). Predictions derived from the binomial mixed-effects model (Table S6.2) using fixed effects only. Dot color encodes predicted precision (0–1); dot size is proportional to OECD urban classification tier.

Discussion

The improvement in Overture Places quality between releases, reflected in large effect sizes for all POI metrics (Cliff's δ = 0.73–0.85), demonstrates that centralized, industry-led conflation can drive systematic quality gains at global urban scale simultaneously. This improvement is, however, attributable primarily to a single source: Meta's internal de-duplication reduced the median co-location stack from 27 to 8 features per city, accounting for essentially all of the positional quality gain. Source diversification, while visible in the 2026 release, remains geographically concentrated in NA, Europe, and ANZ. Urban areas in SSA, LAC and NAWA continue to draw from near-monopoly Meta coverage, leaving those regions structurally dependent on one provider's engineering decisions for future quality trajectories[11,12].

A unifying finding across both themes is that source composition rather than release version or data volume is the dominant predictor of geographic variation in Overture data quality. The April 2026 Overture Buildings dataset lacks attribute information outside OSM-dominated cities. Google, Microsoft, and the EAB dataset together account for 63% of the global urban building inventory, yet carry effectively zero subtype information. Height coverage is more heterogeneous but similarly limited as Google and EAB report near-zero height globally, Microsoft averages 10% (with higher coverage in ANZ), and Esri carries height for approximately 25% of its 2026 contributions, down from 59% in 2024 as newer Esri-sourced buildings entered without the attribute data characteristics of the existing corpus. The negligible effect size for height completeness between releases (Cliff's δ = 0.06) reflects two failures: adding 34 million buildings did not raise aggregate attribute coverage, and height rates of pre-existing pipelines stagnated, indicating no systematic attribute enrichment. This reflects a structural limitation of ML detection: such architectures extract geometry at global scale but yield no semantic attribute richness required for downstream applications[8,27]. The completeness of open building datasets has been shown to correlate with OSM community activity and socioeconomic development indicators[16], and our findings extend this to the attribute domain where ML-sourced footprints inherit geometric coverage but contribute no semantic depth. This gap is compounded by technology companies' documented shift from direct OSM contribution toward proprietary ML-aggregation pipelines[11,12,34], bypassing the community editing feedback loop that generates attribute richness. Conflation pipelines that harmonize these sources at the format level cannot compensate for the upstream absence of semantic labels[11,24]. This source-composition signal extends to the extrinsic domain: in the binomial GLMM, a higher OSM share was associated with greater building completeness, while higher Google and Microsoft shares were associated with lower completeness (Table S6.1). Taken together, these results indicate that Overture's unified schema, while successful in standardizing format and licensing, currently conceals substantial heterogeneity in source quality beneath a single data product. Data users should treat the contributing source as the primary quality diagnostic rather than release version alone. Overture's open-schema architecture and the source-composition framework developed here provide a replicable methodology for evaluating data quality and monitoring progress in future releases.

Regarding limitations, the extrinsic assessment covered 320 cities (~3% of the global urban sample), relying on GLMM extrapolation to unseen countries; grouped cross-validation indicated moderate predictive performance but also revealed non-negligible uncertainty. The study design that compares two data releases captures a single pipeline transition, and whether the trends reported here persist in subsequent releases remains an open question. The source-composition coefficients indicate where building quality in Overture is high, but cannot distinguish the direct effect of OSM-sourced footprints from variation in OSM mapping density and quality[16,35] within each source share. That is, cities with equivalent OSM share but more active mapping communities may show higher completeness than the model predicts.

Closing the building semantic gap will require either systematic integration of authoritative government building registers or advances in AI-based attribute inference capable of annotating ML-detected footprints with functional and structural information. The source-composition framework and quality metrics developed here provide a replicable methodology for monitoring whether future Overture releases achieve such progress.

Methods

Study area

We analyzed the geospatial data quality of Overture Maps releases across all urban settlements identified in the 2025 Global Human Settlement Layer Urban Center [36]. The GHSL-UCDB delineates functional urban areas based on population density thresholds and building surface density, providing a globally consistent, policy-neutral definition of urban extent that avoids administrative boundary inconsistencies common in city-level comparisons. The full dataset encompasses 11,422 urban centers spanning all inhabited continents, stratified into nine world regions following the GHSL regional classification, which modifies the United Nations Sustainable Development Goal (UN SDG) super-regional framework by treating Europe and NA as separate regions (Fig. S5.1).This coverage enabled global inference without geographic selection bias and provided sufficient statistical power for regional comparison across the globe.

Intrinsic quality metrics were computed for the entire extent of each of the 11,422 urban centers in both Overture releases. Extrinsic ground-truth validation was conducted for a stratified subsample of 338 cities selected to represent the full cross-regional and settlement-size distribution of the GHSL.

Data sources

We compared two releases of the Overture Maps Foundation (OMF) dataset:

- **November 2024** (2024-11-13.0, schema v1.3.0): accessed via the Source Cooperative historical mirror, which archives all OMF releases beyond the platform's 60-day retention window. This release was used as the baseline.

- **April 2026** (2026-04-15.0, schema v1.16.0): accessed directly from Overture S3 distribution bucket.

For both releases we used two themes, Places and Buildings. The Places theme provides a global inventory of POIs, with each feature recording a data source identifier, a confidence score, and a hierarchical category assignment drawn from the OMF taxonomy (2,118 leaf categories as of v1.3.0). The Buildings theme provides polygon footprints of the global built environment, with each feature recording its source, and optional attributes including subtype classification, height and floor count. Between the two releases, the total POI inventory grew from approximately 31 million to 42 million features in GHSL areas, and the building inventory grew from 550 million to 585 million features.
The choice of these specific data releases includes a methodologically important interval, namely OMF's first large-scale conflation pipeline update in the April 2026 release which was designed to reduce source duplication and improve attribute completeness. Our study was designed to measure the magnitude and geographic distribution of these improvements.
All data were downloaded as GeoParquet files and processed locally using DuckDB 1.5.1 with the spatial extension. City assignment for all 11,422 urban centers used H3 discrete global grid system cells at resolution 9 as a pre-computed spatial lookup key, avoiding repeated polygon-in-polygon joins across the full dataset[37] (See Supplementary Material §2 for full download and indexing procedure). An overview of the full data processing and analysis pipeline is shown in Fig. S2.1.

Quality framework

We followed the ISO 19157 geographic data quality framework (ISO, 2013), which distinguishes between intrinsic quality indicators, i.e. self-referential measures derivable from the dataset itself without an external reference, and extrinsic indicators that require comparison against an independent ground truth. Intrinsic assessment covered the entire areas of all 11,422 cities across both releases, while extrinsic assessment was conducted for the 338-city stratified subsample through manual building counts against background imagery. This two-tier design reflects the practical constraints of global-scale quality auditing: intrinsic metrics provide comprehensive spatial coverage, while extrinsic metrics provide interpretive calibration for the regions where they are available. The full set of analysis tasks, their quality dimensions, and their coverage are summarized in Table S1.1.

Intrinsic quality metrics

POI source diversity (P-01)

Intrinsic metrics were computed for all 11,422 urban centers across both releases using DuckDB 1.5.1 with the spatial extension. For each metric, city-level values were first computed and then aggregated along two independent dimensions: by world region, to characterize the global spatial distribution of quality, and by primary data source, to identify provider-level

differences in data quality. The city is therefore the unit of observation throughout. Regional and source summaries are derived from the same city-level base.

We quantified the diversity of data sources contributing POIs to each city (P-01) using Shannon entropy and its normalized form, the Pielou's evenness index. For a city with *S* source contribution proportions $p_1, p_2, \ldots, p_S$, Shannon entropy is $H = -\Sigma p_{\mathrm{i}} \cdot ln(p_{\mathrm{i}})$. Pielou's Evenness is then $E = H/ln\,(S)$ where $E \in [0,1]$ with ***E***=1 indicating perfectly uniform source contributions and *E* approaching 0 indicating near-complete dominance by a single source. We report *E* as the primary source diversity indicator, because it is independent of *S*, enabling fair comparison across cities with different numbers of contributing sources. The number of sources *S* was reported as a complimentary richness indicator. Both metrics were computed at the city level and are displayed in Fig. 1 (color = *E*, dot size = *S*).

POI co-location (P-02)

Co-location was defined as two or more POIs sharing an identical coordinate pair within a city (P-02). This pattern is a diagnostic signature of bulk data duplication and lower data quality as distinct real-world entities usually don't share the same physical 2D location. While exceptions exist (e.g. high-rise buildings), overlapping POIs are less useful for downstream applications. We consider co-locating POIs a positional accuracy failure under ISO 19157. For each city, we computed the fraction of POIs that shared their coordinate with at least one other POI, and separately recorded the maximum co-location stack depth (the largest number of POIs sharing a single coordinate pair). Both statistics were computed for each data source independently, enabling identification of the contributing providers responsible for co-located records. City-level co-location rates were then displayed in Fig. 2.

POI category quality (P-03)

We characterized the thematic completeness and specificity of POI category assignment using two complimentary indicators (P-03). First, the percentage of POIs assigned no primary category at all captured the most severe form of thematic incompleteness. Second, the specificity score (S_k) quantified how precisely categorized POIs were within the OMF's six level taxonomy. For a POI assigned a taxonomy level *k* within branch *b*, the score is computed as:

$$S_{\mathrm{k}} = log(1 + \Sigma_{\mathrm{l=2}}{}^{\mathrm{k}} n_{\mathrm{l}})/log\,(1 + \Sigma_{\mathrm{l=2}}{}^{\mathrm{L}} n_{\mathrm{l}})$$

Where n_l is the number of taxonomy members at level *l* within branch *b*, and *L* is the maximum depth of that branch. The logarithmic normalization scales the cumulative counts to a normalized range between 0 and 1, where 0 corresponds to the least specific assignment, that is, only the top-level category is known, and 1 corresponds to the deepest available classification within a branch. Mean S_k was computed for each city from all categorized POIs and then aggregated to regional medians. The OMF category taxonomy was stable between the two releases with no structural changes, ensuring that S_k values are comparable across years.

Building source diversity (B-01) and attribute completeness (B-02)

Building source composition was characterized using the same Shannon/Pielou framework as for POI analysis. The dominant contributing source per city, determined as the source supplying the majority of building footprints, was mapped globally in Fig. 3. Attribute completeness (B-02) was measured as the percentage of buildings with non-null values for three semantically important fields: subtype (coarse occupancy classification), height (meters above ground), and num_floors (building level count). These three attributes collectively determine whether a building footprint can support downstream applications in urban analytics, energy modeling and population estimation.

Building geometric overlap (B-03)

Geometric overlap between building footprints was measured as the percentage of each building's polygon area that intersected the polygon of at least one other building in the same city, independent of the amount of overlap. Overlapping footprints are geometrically impossible in the physical world. They arise from imperfect data fusion or digitization. The overlap fraction was computed for every building pair within each city using a spatial self-join (*ST_Intersects*) followed by *ST_Intersection*, constrained to within-city pairs to manage computational costs. Per building fractions were averaged to produce a city-level mean overlap rate (Fig. S1.4), and then aggregated to regional medians.

Extrinsic (ground-truth) building completeness assessment

Sampling design

Extrinsic validation was conducted for a stratified sample of 338 cities drawn from the 2025 GHSL dataset to represent the full range of world regions and settlement sizes present in the global urban hierarchy. Cities were classified by population into four size strata: Small Urban Areas (50,000–200,000), Medium-Size Urban Areas (200,000–500,000), Metropolitan Areas (500,000–1.5 million), and Large Metropolitan Areas (>1.5 million). Nine reporting regions were defined, separating Europe from NA rather than merging them under the standard eight-region SDG classification (Fig. S5.1.). With the exception of Oceania, each region contributed 40 cities (10 per size stratum). ANZ could not be fully stratified because only 44 eligible cities exist in the GHSL, resulting in a non-uniform stratum distribution (30 small urban areas, 3 medium-size, 4 metropolitan, 3 large metropolitan). Oceania contributed all 18 of its available GHSL cities, none of which reached metropolitan size. Because this constitutes the full population of eligible cities rather than a sample, and because of the absence of larger city-size classes, Oceania was excluded from the regression analyses, leaving 320 cities for statistical modelling (Supplementary Materials Section 5).

Sampling zone definition

For the manual analysis, buildings were extracted from standardized analysis zones within each of the 320 sampled cities. The geometry of sub-areas used for sampling were centered on a representative point guaranteed to be within each city boundary, generated with GeoPandas.

This location was then defined in the Icosahedral Snyder Equal Area Aperture 4 Hexagonal (ISEA4H) discrete global grid system (DGGS) at a fixed resolution (Level 14) that results in spatially unbiased areas for global comparison. The analysis zone was defined as the single ISEA4H hexagonal cell at Level 14 with an approximate size of 0.19 km². This approach produced an average of 226 (median: 163) mapped buildings per city.

Manual assessment protocol

Within each analysis zone, building footprints from the April 2026 Overture release were overlaid on sub-meter commercial satellite imagery. An experienced analyst visually inspected each city and recorded the count of: (i) buildings visible in imagery but absent from Overture (omissions, false negatives, *FN*); (ii) Overture footprints with no corresponding real-world structure visible (commissions, false positives, *FP*); and (iii) buildings correctly mapped by both sources (true positives, *TP*). From these counts, completeness was derived as $TP/(TP + FN)$ and precision as $TP/(TP + FP)$ for each city.

Variation in city-level completeness and precision was then modelled using two binomial generalized linear mixed models (GLMMs) with a logit link (i.e. one for each outcome). Fixed effects included world region, city population density, settlement size class, and source composition. The latter was expressed as four isometric log-ratio (ILR) coordinates derived from the five contributing source shares (OpenStreetMap, Microsoft, Google, EAB, and an aggregated other category), transforming the compositional predictors into an unconstrained orthonormal basis that avoids the collinearity inherent in raw proportions. A random intercept for country was included in both models to account for the within-country clustering of sampled cities. Model coefficients are reported as odds ratios ($= e^{\beta}$), interpreted as the multiplicative change in the odds of completeness or precision associated with a one-unit change in each predictor.

Statistical analysis and reporting

All regional summaries were computed as the median and mean of city-level values within each region and data release, where the median is the primary reported statistic and the mean is provided in parentheses for reference. This convention is applied uniformly across all metrics and tables to support direct comparison across sections. Using city-level data as the unit of aggregation gives each urban area equal weight regardless of its POI or building count, preventing the largest cities from dominating regional statistics.

Release-to-release change was characterized using the absolute difference in regional medians and means (Δ). Because city-level quality metrics follow right-skewed distributions bounded at zero, release-to-release changes are evaluated using Cliff's delta[38], a distribution-free effect size based on the proportion of cities recording an improvement.

Data availability

The Overture Maps Foundation building and place datasets analysed in this study are publicly available via Source Cooperative, which provides permanent archiving of all Overture releases. The November 2024 release (2024-11-13.0, schema v1.3.0) is available at https://source.coop/fused/overture/2024-11-13-0; the April 2026 release (2026-04-15.0, schema v1.16.0) is available at https://source.coop/fused/overture/2026-04-15-0. The GHSL Urban Centre Database 2025 used to define urban study areas is available at https://data.europa.eu/doi/10.2760/3046391 [36]. The city-level intrinsic quality metrics derived in this study for all 11,422 GHSL urban areas (both releases), the H3 and ISEA4H spatial index files, and the ground-truth building completeness and precision validation records for the 338 sampled cities are deposited at Zenodo: https://doi.org/10.5281/zenodo.22114268 [39].

Code availability

All code used for data download, preprocessing, analysis and the generation of figures and tables is publicly available via GitHub at https://github.com/gatorlab-geo/overture-qa and via Zenodo at https://doi.org/10.5281/zenodo.22114268.

References

1. *World Urbanization Prospects: The 2018 Revision*. 123p https://digitallibrary.un.org/record/3833745 (2019).
2. Balland, P.-A. *et al.* Complex economic activities concentrate in large cities. *Nat Hum Behav* **4**, 248–254 (2020).
3. Fang, C. & Yu, D. Urban agglomeration: An evolving concept of an emerging phenomenon. *Landscape and Urban Planning* **162**, 126–136 (2017).
4. Psyllidis, A. *et al.* Points of Interest (POI): a commentary on the state of the art, challenges, and prospects for the future. *Comput.Urban Sci.* **2**, 20 (2022).
5. Huang, B. & Wang, J. Big spatial data for urban and environmental sustainability. *Geo-spatial Information Science* **23**, 125–140 (2020).
6. Biljecki, F. & Chow, Y. S. Global Building Morphology Indicators. *Computers, Environment and Urban Systems* **95**, 101809 (2022).
7. Deparday, V., Cowan, N. M., Doherty, G. A., Gupta, M. L. & Soden, R. J. *Open Cities Africa : Program of the GFDRR Open Data for Resilience Initiative*. (2020).

8. Boo, G. *et al.* High-resolution population estimation using household survey data and building footprints. *Nat Commun* **13**, 1330 (2022).
9. Goodchild, M. F. Citizens as Voluntary Sensors: Spatial Data Infrastructure in the World of Web 2.0 (Editorial). *International Journal of Spatial Data Infrastructures Research (IJSDIR)* **2**, 24–32 (2007).
10. Senaratne, H., Mobasheri, A., Ali, A. L., Capineri, C. & Haklay, M. (Muki). A review of volunteered geographic information quality assessment methods. *International Journal of Geographical Information Science* **31**, 139–167 (2017).
11. Ochoa-Ortiz, H. & Re, B. Exploring why and how commercial organizations contribute to OpenStreetMap. *Annals of GIS* **31**, 221–232 (2025).
12. Schröder-Bergen, S., Michel, B., Glasze, G. & Dammann, F. Open Geospatial Data within Digital Capitalism: OpenStreetMap and the Overture Maps Foundation. *Cartographica* **60**, 160–172 (2025).
13. Prioleau, M. Overture Maps Foundation: Making Open Data the Winning Choice. *Overture Maps Foundation* https://overturemaps.org/blog/2025/overture-maps-foundation-making-open-data-the-winning-choice/ (2025).
14. Haklay, M. & Weber, P. OpenStreetMap: User-Generated Street Maps. *IEEE Pervasive Computing* **7**, 12–18 (2008).
15. Glasze, G. & Perkins, C. Social and Political Dimensions of the OpenStreetMap Project: Towards a Critical Geographical Research Agenda. in *OpenStreetMap in GIScience: Experiences, Research, and Applications* (eds Jokar Arsanjani, J., Zipf, A., Mooney, P. & Helbich, M.) 143–166 (Springer International Publishing, Cham, 2015). doi:10.1007/978-3-319-14280-7_8.
16. Herfort, B., Lautenbach, S., Porto de Albuquerque, J., Anderson, J. & Zipf, A. A spatio-temporal analysis investigating completeness and inequalities of global urban building data in OpenStreetMap. *Nat Commun* **14**, 3985 (2023).

17. Zhou, Q., Zhang, Y., Chang, K. & Brovelli, M. A. Assessing OSM building completeness for almost 13,000 cities globally. *International Journal of Digital Earth* **15**, 2400–2421 (2022).
18. Ullah, T., Lautenbach, S., Herfort, B., Reinmuth, M. & Schorlemmer, D. Assessing Completeness of OpenStreetMap Building Footprints Using MapSwipe. *ISPRS International Journal of Geo-Information* **12**, 143 (2023).
19. Hochmair, H. H., Juhász, L. & Cvetojevic, S. Data Quality of Points of Interest in Selected Mapping and Social Media Platforms. in *Progress in Location Based Services 2018* (eds Kiefer, P., Huang, H., Van de Weghe, N. & Raubal, M.) vol. Lecture Notes in Geoinformation and Cartography 293–313 (Berlin, Springer, 2018).
20. Milias, V. & Psyllidis, A. Assessing the influence of point-of-interest features on the classification of place categories. *Computers, Environment and Urban Systems* **86**, 101597 (2021).
21. Yeow, L. W., Low, R., Tan, Y. X. & Cheah, L. Point-of-Interest (POI) Data Validation Methods: An Urban Case Study. *ISPRS International Journal of Geo-Information* **10**, 735 (2021).
22. Mülligann, C., Janowicz, K., Ye, M. & Lee, W.-C. Analyzing the Spatial-Semantic Interaction of Points of Interest in Volunteered Geographic Information. in *Spatial Information Theory* (eds Egenhofer, M., Giudice, N., Moratz, R. & Worboys, M.) 350–370 (Springer, Berlin, Heidelberg, 2011). doi:10.1007/978-3-642-23196-4_19.
23. Barron, C., Neis, P. & Zipf, A. A Comprehensive Framework for Intrinsic OpenStreetMap Quality Analysis. *Transactions in GIS* **18**, 877–895 (2014).
24. Florio, P. *et al.* Towards a Pan-EU building footprint map based on the hierarchical conflation of open datasets: the digital building stock model - DBSM. *The International Archives of the Photogrammetry, Remote Sensing and Spatial Information Sciences* **XLVIII-4-W7-2023**, 47–52 (2023).

25. Oostwegel, L. J. N., Schorlemmer, D. & Guéguen, P. From Footprints to Functions: A Comprehensive Global and Semantic Building Footprint Dataset. *Sci Data* **12**, 1699 (2025).
26. Ballantyne, P. & Berragan, C. Overture Point of Interest data for the United Kingdom: A comprehensive, queryable open data product, validated against Geolytix supermarket data. *Environment and Planning B: Urban Analytics and City Science* **51**, 1974–1980 (2024).
27. Gevaert, C. M., Buunk, T. & van den Homberg, M. J. C. Auditing Geospatial Datasets for Biases: Using Global Building Datasets for Disaster Risk Management. *IEEE Journal of Selected Topics in Applied Earth Observations and Remote Sensing* **17**, 12579–12590 (2024).
28. Maneepong, K. *et al.* Towards High-Resolution Population Mapping: Leveraging Open Data, Remote Sensing, and AI for Geospatial Analysis in Developing Country Cities—A Case Study of Bangkok. *Remote Sensing* **17**, 1204 (2025).
29. Foursquare. OS Places. https://opensource.foursquare.com/os-places/ (2026).
30. AllThePlaces. All The Places. https://alltheplaces.xyz/ (2026).
31. Sirko, W. *et al.* Continental-Scale Building Detection from High Resolution Satellite Imagery. *arXiv.org* https://arxiv.org/abs/2107.12283v2 (2021).
32. Microsoft. GlobalMLBuildingFootprints. https://github.com/microsoft/GlobalMLBuildingFootprints (2026).
33. Shi, Q. *et al.* The Last Puzzle of Global Building Footprints—Mapping 280 Million Buildings in East Asia Based on VHR Images. *Journal of Remote Sensing* **4**, 0138 (2024).
34. Tockner, L., Herfort, B., Lautenbach, S. & Zipf, A. Corporate mapping in OpenStreetMap – shifting trends in global evolution and small-scale effects. *Geo-spatial Information Science* **29**, 489–508 (2026).
35. Haklay, M. How good is Volunteered Geographical Information? A comparative study of OpenStreetMap and Ordnance Survey datasets. *Environment and Planning B: Planning and Design* **37**, 682–703 (2010).

36. Melchiorri, M *et al. Stats in the City: The GHSL Urban Centre Database 2025 : Public Release GHS UCDB R2024*. https://data.europa.eu/doi/10.2760/3046391 (2024) doi:10.2760/3046391.

37. Juhász, L. Accelerating Point-in-Polygon Predicates via Algebraic Hash-Joins and Discrete Global Grids at Scale: An Interactive Benchmark. in *The 34th ACM International Conference on Advances in Geographic Information Systems* (ACM, Riverside, CA, USA, 2026). doi:10.1145/3841645.3843101.

38. Cliff, N. Dominance statistics: Ordinal analyses to answer ordinal questions. *Psychological Bulletin* **114**, 494–509 (1993).

39. Juhász, L. gatorlab-geo/overture-qa: v1.0.0 — Initial release. https://doi.org/10.5281/zenodo.22114268 (2026) doi:10.5281/zenodo.22114268.

Competing interests

The authors declare no competing interests.

Funding

This research received no external funding.

Contributions

Conceptualization: L.J., H.H.H. **Data curation**: L.J., H.H.H. **Formal analysis**: L.J. (intrinsic), H.H.H. (extrinsic). **Methodology**: L.J., H.H.H. **Software**: L.J., H.H.H. **Validation**: L.J., H.H.H. **Visualization**: L.J. **Writing – original draft**: L.J., H.H.H. **Writing – review & editing**: L.J., H.H.H.

Supplementary Files

This is a list of supplementary files associated with this preprint. Click to download.

- JuhaszHochmairSciRepOvertureSUPPLEMENTARYunlink1.pdf